Enhancer RNAs are necessary and sufficient for activity-dependent neuronal gene transcription

Nancy V.N. Gallus[1], Rhiana C. Simon[1], Aaron J. Salisbury[1], Jasmin S. Revanna[1], Kendra D. Bunner[1], Katherine E. Savell[1], Faraz A. Sultan[1], Charles A. Gersbach[2], & Jeremy J. Day[1]*

[1]Department of Neurobiology, University of Alabama at Birmingham, Birmingham, AL 35294, USA
[2]Department of Biomedical Engineering, Duke University, Durham, NC 27708, USA.

*Corresponding authors

Distal enhancer elements in DNA enable higher-order chromatin interactions that facilitate gene expression programs and thus contribute to cellular phenotype and function. In the brain, enhancer-promoter interactions help to ensure cell- and tissue-specific gene expression profiles, defining which genes are active during neuronal specification and which genes remain accessible in adult neurons. In addition to their close links to gene activation, enhancer elements themselves are subject to widespread, bidirectional transcription that yield non-coding enhancer RNA (eRNA). However, although eRNAs are correlated with overall enhancer activity, the precise function of eRNAs remains controversial. Here, we examined the function of eRNAs arising from multiple enhancers near the well-characterized immediate early gene *Fos* (also known as *c-Fos*). We show that eRNA transcription from *Fos* enhancers is dynamically modulated by various forms of neuronal activity, requires RNA polymerase II, and precedes activity-dependent induction of *Fos* mRNA. Visualization of *Fos* eRNA transcripts on a single cell level using single molecule fluorescent *in situ* hybridization revealed localization within the cell nucleus. Anti-sense based *Fos* eRNA knockdown decreased *Fos* mRNA expression, whereas mRNA knockdown did not affect eRNA levels. Targeted stimulation of eRNA synthesis from *Fos* enhancers using CRISPR-dCas9 fusion proteins produced corresponding increases in *Fos* mRNA expression, with limited cross-talk between enhancers. Similarly, CRISPR-targeted delivery of eRNA to a *Fos* enhancer elevated mRNA induction following neuronal depolarization. Finally, we show that anti-sense based knockdown of a single *Fos* eRNA is sufficient to alter neuronal physiology. Together, these results suggest that RNAs transcribed from neuronal enhancers are important regulators of enhancer-driven gene regulatory programs and neuronal function.

To orchestrate the precise gene expression patterns that give rise to the phenotypic and functional diversity of complex biological systems, mammalian genomes utilize millions of regulatory elements known as enhancers. These enhancers, often located many kilobases from genes that they regulate, direct transcriptional dynamics at linked genes by activation of proximal gene promoters (Heinz et al., 2015; Li et al., 2016; Wang et al., 2011). Enhancer-promoter interactions help to ensure the exquisite specificity of cell- and tissue-specific gene expression profiles in the brain, defining which genes can be turned on during neuronal specification and which genes remain accessible in adult neurons (Gray et al., 2015; Nord et al., 2013). In addition to regulating neuronal development, enhancer regions direct activity- and experience-dependent gene expression programs required for neuronal plasticity, memory formation, and behavioral adaptation to environmental stimuli (Joo et al., 2016; Kim et al., 2010; Malik et al., 2014; Schaukowitch et al., 2014; Telese et al., 2015). Moreover, the vast majority of DNA sequence variants that possess a causal relationship to neuropsychiatric disease and intellectual disability fall in non-coding regions of DNA (Davidson et al., 2011; Eckart et al., 2016; Edwards et al., 2012; Gordon and Lyonnet, 2014; Inoue and Inoue, 2016; Network and Pathway Analysis Subgroup of Psychiatric Genomics, 2015; Roussos et al., 2014; Schizophrenia Working Group of the Psychiatric Genomics, 2014; Vermunt et al., 2014; Voisin et al., 2015; Yao et al., 2015), and these variants are increasingly becoming linked to altered enhancer function. Thus, understanding how genomic enhancers regulate individual genes in neuronal systems is critical for unraveling transcriptional contributions to brain health and disease.

Recent advances in DNA sequencing have revealed that the transcriptional landscape of all mammalian organisms is far more complex than previously appreciated. In contrast to earlier predictions, a significant fraction of mammalian

genomes is transcribed into non-coding RNAs, which include long non-coding RNAs (lncRNAs; generally defined as non-coding RNAs longer than 200 nucleotides) (Djebali et al., 2012; Hangauer et al., 2013; Quinn and Chang, 2016). Much of this lncRNA landscape is dedicated to enhancer regions which undergo bidirectional, RNA polymerase II (RNAP2)-dependent transcription to yield enhancer RNAs (eRNAs) that are generally not spliced or polyadenylated (Arner et al., 2015; Gray et al., 2015; Kim et al., 2015; Kim et al., 2010; Kim and Shiekhattar, 2015). Critically, RNA synthesis from enhancers that regulate cellular differentiation and responses to cellular activation occurs *prior* to mRNA synthesis from linked genes (Arner et al., 2015), and also *prior* to important chromatin remodeling events that are generally used to identify enhancers (Kaikkonen et al., 2013). In addition, eRNA transcription from enhancers is highly correlated with overall e nhancer activity and the presence of enhancer-promoter loops (Li et al., 2016; Sanyal et al., 2012). In neuronal systems, eRNAs arising from activity-dependent enhancers are pervasively transcribed in response to neuronal activation, plasticity-inducing stimulation, and behavioral experience (Joo et al., 2016; Kim et al., 2010; Malik et al., 2014; Schaukowitch et al., 2014; Telese et al., 2015), providing a key link between enhancers and the downstream gene expression programs that regulate brain function.

Although recent reports suggest a functional role for eRNAs in regulation of enhancer states, the specific nature of this role is controversial. Here, we investigate eRNA transcription from neurons genome-wide as well as eRNA synthesis, localization, and function from well-characterized enhancers near the *Fos* gene. This immediate-early gene is broadly responsive to neuronal activity in the brain, and enhancers at this gene contribute to distinct activity-dependent induction dynamics of *Fos* mRNA (Fleischmann et al., 2003; Joo et al., 2016; Kim et al., 2010; Malik et al., 2014; Savell et al., 2016; Zovkic et al., 2014). We provide four lines of novel converging evidence supporting a critical functional role of eRNAs in neuronal systems. We show that activity-induced expression of eRNAs from enhancers is significantly correlated with expression from nearby activity-responsive genes across the genome, that *Fos* eRNAs are localized to distinct loci within the nucleus, that transcriptional activation of *Fos* enhancers drives activation of *Fos* mRNA, and that eRNAs from a distal *Fos* enhancer are both necessary and sufficient for activity-regulated induction of *Fos* mRNA. Finally, we confirm the relevance of eRNAs in neuronal function by demonstrating that altered levels of a single eRNA can lead to decreased neuronal firing.

Results

Neuronal stimulation reveals activity-dependent enhancer RNAs

To map neuronal eRNAs across the rat genome, we took advantage of the fact that eRNAs are predominantly non-polyadenylated transcripts. Using a recently published non-PolyA RNA-seq dataset from rat cortical neuron cultures (Savell et al., 2016), we quantified 12,924 regions of contiguous non-PolyA transcription that fell >1kb outside of annotated gene boundaries, consistent with common cutoffs used to dissociate enhancers from more proximal promoters (**Fig. 1A**). To ensure that these transcribed regions were in fact enhancers, we utilized publicly available ENCODE datasets from adult mouse cortex for the major histone modifications associated with enhancer loci (H3K4me1, H3K4me3, and H4K27ac). Of 12,924 transcribed intergenic regions (TIRs), 3,107 regions overlapped H3K4me1 peaks (a mark of active enhancers (Li et al., 2016)) or overlapped both H3K4me3 and H4K27ac peaks (marks often used to denote poised enhancers (Li et al., 2016)). These transcribed regions, which we designated as transcriptionally active enhancers (TAEs; **Fig. 1A-B**) exhibited increased levels of non-polyA RNA expression as compared to non-enhancer TIRs (data not shown), and were also enriched for RNA Polymerase II (RNAP2) and the enhancer-linked chromatin looping factor CTCF (CCCTC-binding factor) (**Fig. 1B**). DNA sequences at these locations exhibited elevated sequence conservation and overlap with CpG islands, regions which generally lack DNA methylation (another cardinal feature of enhancers).

To determine whether eRNAs are correlated with activity-dependent alterations in protein-coding genes, we examined non-PolyA RNA transcription from TAEs following neuronal depolarization with 25mM potassium chloride (KCl). This allowed us to investigate both eRNA and mRNA expression (from distinct PolyA+ RNA datasets) changes in response to neuronal depolarization. We identified over 230 genes (termed immediate early genes, or IEGs;

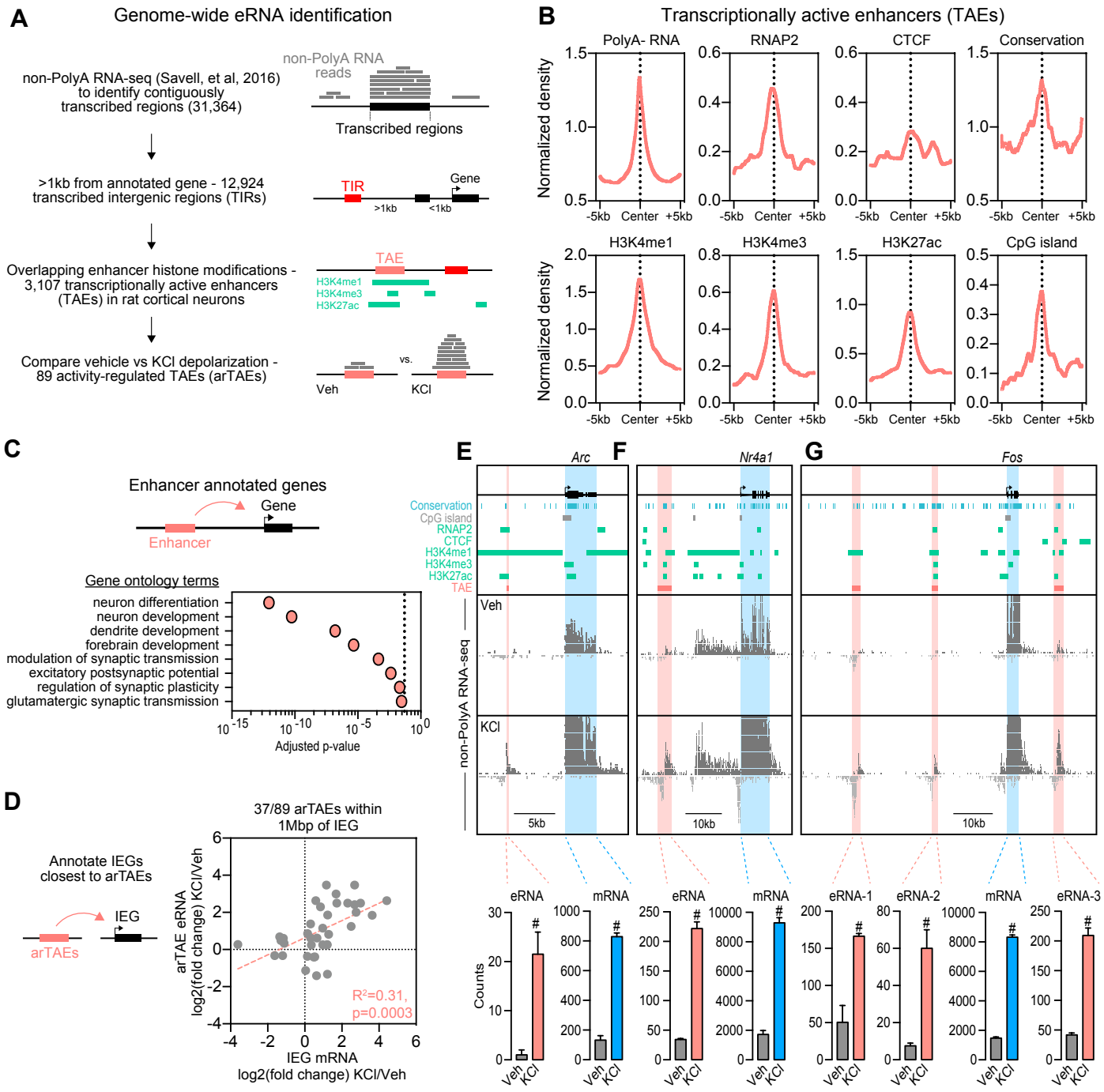

Figure 1. Genome-wide characterization of eRNAs. **A**, Analysis pipeline for localization and quantification of transcriptionally active enhancers (TAEs), and genome-wide comparisons of eRNA expression following neuronal depolarization. Non-PolyA RNA-seq datasets from previous publication using cultured rat cortical neurons (Savell, et al., 2016) were used to identify contiguously transcribed regions, which were filtered to remove transcribed regions overlapping annotated genes. Of 12,924 transcribed intergenic regions (TIRs), 24% (3,107 loci) overlapped histone modifications consistent with active or poised enhancers, and were designated TAEs. Of these, 89 met genome-wide criteria for differential expression following 1hr neuronal depolarization with 25mM potassium chloride (KCl), and were designated activity-regulated TAEs (arTAEs). **B**, Transcriptionally active enhancers exhibit elevated RNAP2 occupancy, CTCF binding, sequence conservation (phastCons13way score), histone modifications (H3K4me1, H3K4me3, H3K27ac), and CpG island density as compared to surrounding regions. Chromatin immunoprecipitation datasets were obtained from the adult mouse cortex (ENCODE project) and lifted over to the rat Rn5 genome assembly. **C**, Gene ontology for 1,362 unique genes closest to TAEs. TAEs are enriched near genes that regulate neuronal function and synaptic transmission. **D**, eRNA-mRNA pairs were determined by annotation of closest immediate early genes (IEGs) induced by neuronal depolarization with 25mM KCl, with a 1Mbp distance cutoff. Correlation between differential expression of IEG mRNAs following KCl depolarization and differential expression of eRNA from closest arTAEs following depolarization. Values are expressed as log2(fold change) of eRNA or mRNA counts used for comparison in DESeq2. Correlation determined with linear regression. **E-G**, Top, Genome browser tracks showing Non-PolyA RNA expression at three KCl-regulated IEGs (*Arc*, *Nr4a1*, and *Fos*), relative to tracks marking conserved DNA elements, CpG islands, RNAP2 and CTCF binding, and enhancer-linked histone modifications. Our pipeline identified one or more TAEs near each IEG. Bottom, RNA-seq count quantification of transcripts from TAEs (eRNAs, from non-PolyA libraries), and mRNAs (from separate PolyA+ libraries). #FDR < 0.05 for DeSeq2 comparison of differential expression between vehicle and KCl groups.

Supplementary Data Table 1) and 89 TAEs (termed activity-regulated TAEs, or arTAEs) that were significantly altered by KCl treatment. Gene-ontology analysis revealed an enrichment in terms associated with neurodevelopment, synapse dynamics, and overall neuronal function for genes adjacent to our TAE (**Fig. 1D)**. To examine correlations in depolarization-induced changes at individual eRNA-mRNA pairs, we annotated the nearest IEG (within 1Mbp) to each of the 89 arTAE loci (**Fig. 1C**; **Supplementary Data Table 2**). 42% of arTAEs met this criterion, and at these loci, activity-induced expression of eRNAs and mRNAs were significantly correlated. **Figure 1E-G** shows non-PolyA RNA-seq results from three representative IEGs (*Arc*, *Nr4a1*, and *Fos*) that are significantly induced by KCl depolarization. Each of these genes displayed distal arTAEs, including at least 3 distinct enhancers near the *Fos* gene. The locations of these enhancers are consistent with locations of enhancer elements in other species relative to the *Fos* gene (Joo et al., 2016; Kim et al., 2010), and map to DNA sequences that are enriched for RNAP2 and histone modifications associated with active enhancers (H3K4me1 and H3K27ac). Further, each of these elements undergoes bidirectional transcription to yield strand-specific eRNAs.

To determine whether *Fos* eRNAs are sensitive to other forms of neuronal and synaptic activation or inactivation, DIV 11 cortical neurons were stimulated with specific glutamate receptor agonists (AMPA and NMDA), the adenylyl cyclase activator Forskolin, or inactivated with the sodium channel blocker tetrodotoxin (TTX) (**Fig. 2A**). Enhancer RNA transcribed from the most distal *Fos* enhancer (termed *Fos* enhancer-1 or E1) was increased by KCl, AMPA, NMDA, and Forskolin in a dose-dependent fashion. Likewise, *Fos* eRNA-1 levels were reduced by TTX, suggesting that eRNA levels at this gene are bidirectionally modulated by neuronal activity states. To further explore this relationship, we performed a KCl stimulation time-course experiment in which cultured neurons were depolarized with KCl and RNA was isolated from neurons at multiple timepoints (15, 30, 45, and 60 min) after treatment. These results revealed that *Fos* eRNA-1 is upregulated as soon as 15 min following KCl depolarization, whereas *Fos* mRNA is not significantly upregulated until 30 min after stimulation (**Fig. 2B**). Moreover, *Fos* eRNA expression plateaus at 45 min after neuronal depolarization, whereas *Fos* mRNA levels continue to rise. These results indicate *Fos* eRNA is induced prior to *Fos* mRNA following neuronal activation and confirm previously described dynamics of eRNA transcription (Schaukowitch et al., 2014; Arner et al., 2015).

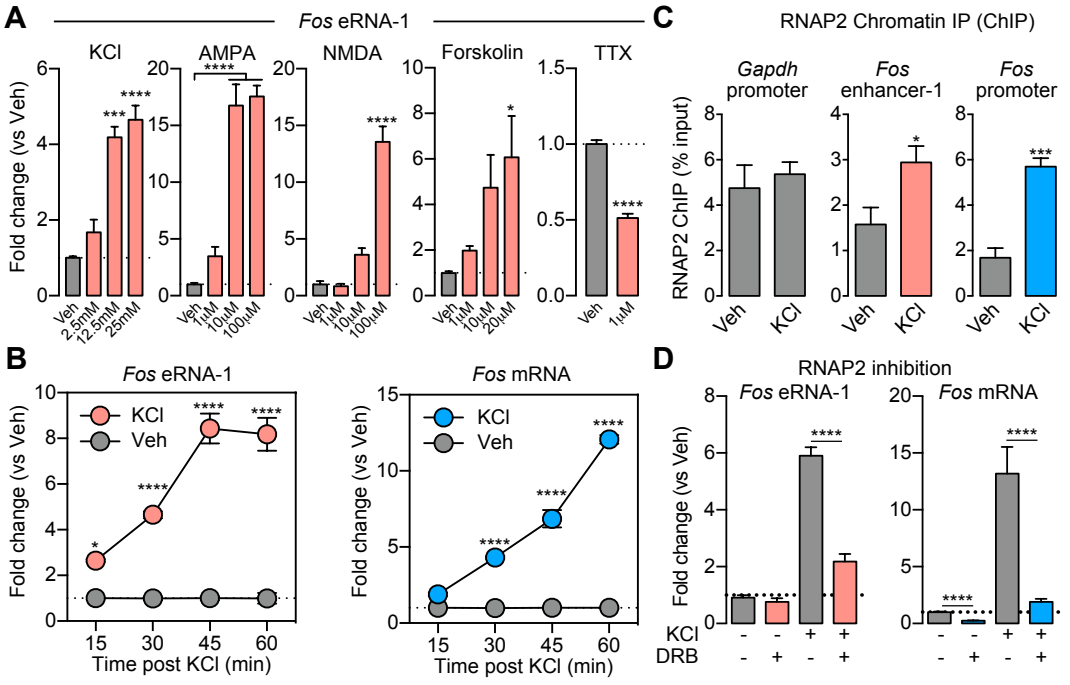

Figure 2. Activity-dependence and synthesis of *Fos* eRNAs. **A**, RT-qPCR analysis of eRNA-1 expression in response to 1h treatment with KCl, AMPA, NMDA, and Forskolin reveals activity dependent induction of *Fos* eRNA-1, while TTX treatment resulted in decreased *Fos* eRNA-1 expression (one-way ANOVA for KCl $F(3,8)=39.05$, $p<0.0001$, AMPA $F(3,8)=59.04$, $p<0.0001$, NMDA $F(3,8)=61.87$, $p<0.0001$, FSK $F(3,8)=4.132$, $p<0.05$, with Dunnette's post hoc test for multiple comparisons, and unpaired t-test for TTX $t(10)=12.83$, $p<0.0001$). **B**, *Fos* eRNA-1 is upregulated at 15min and peaks after 45min of KCl treatment (two-way ANOVA with main effect of KCl, $F(3,15)=35.4$, $p<0.0001$, Sidak's post hoc test for multiple comparison). In contrast, *Fos* mRNA is induced within 30min and does not plateau within the 60min time course (two-way ANOVA, $F(3,16)=169.2$, $p<0.0001$, Sidak's post hoc test for multiple comparison). **C**, RNAP2 CHIP reveals increased recruitment of RNAP2 to the *Fos* enhancer-1 and *Fos* promoter after KCl-mediated depolarization (unpaired t-test, for enhancer-1 $t(6)=2.651$, $p<0.05$, and promoter $t(6)=7.812$, $p<0.001$). **D**, 2h pre-treatment with RNAP2 dependent transcription inhibitor DRB prior to 1h KCl treatment blocked KCl mediated induction of *Fos* eRNA-1 and mRNA (two-way ANOVA, with main effect of DRB $F(1,42)=34.15$, $p<0.0001$, and $F(1,41)=84.64$, Tukey's post hoc test for multiple comparison). Data expressed as mean ± s.e.m. Multiple comparisons, *p<0.05, **p<0.01, ***p<0.001, ****p<0.0001.

To examine the mechanisms

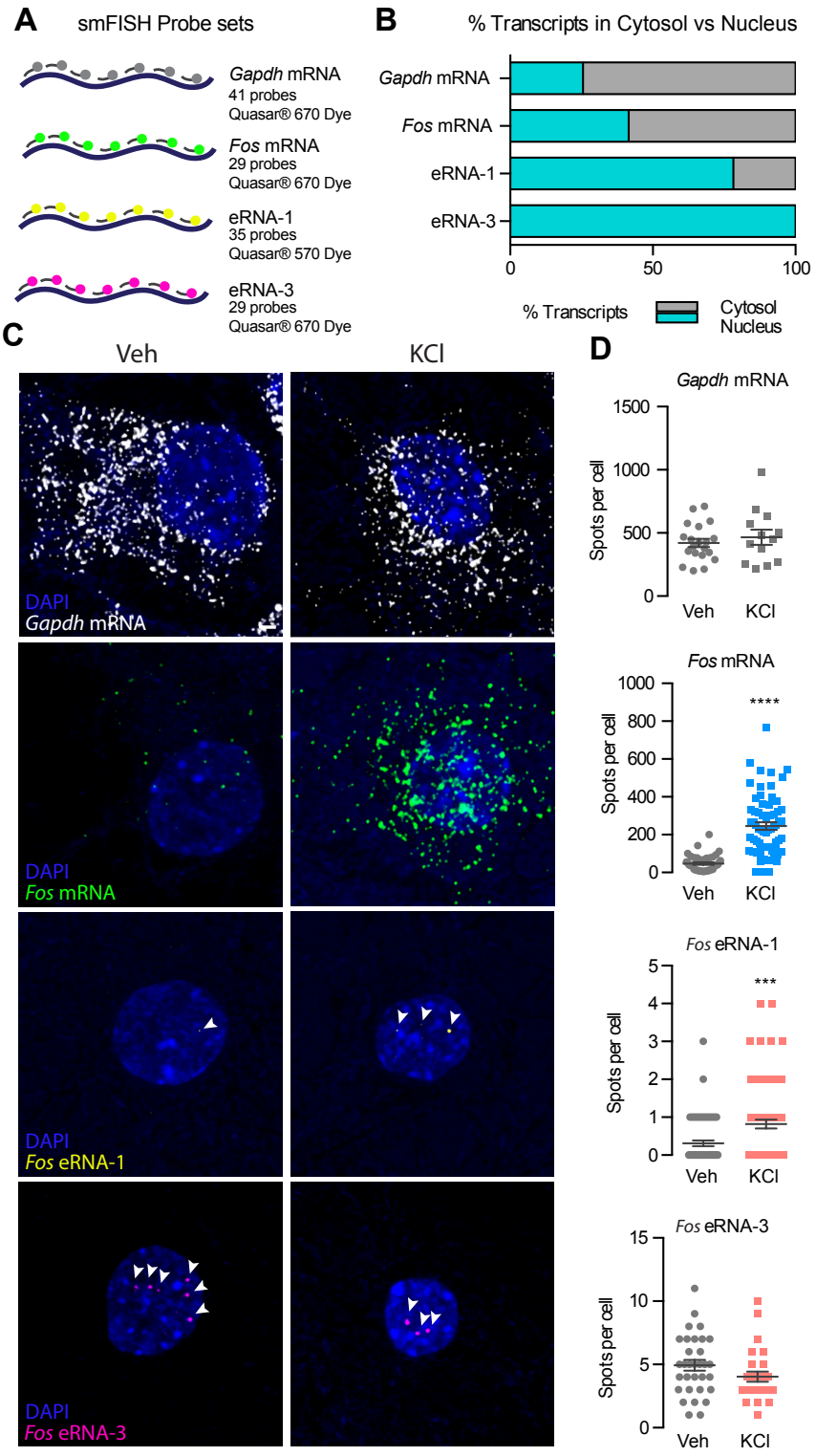

Figure 3. Cellular localization of *Fos* eRNA and mRNA. **A**, Illustration of smFISH probe sets indicating number of probes, dye, and LUT. **B**, Quantification of smFISH for *Gapdh* mRNA, *Fos* mRNA, *Fos* eRNA-1 and *Fos* eRNA-3 transcripts in the cytosol vs nucleus. **C**, smFISH for *Gapdh* mRNA, *Fos* mRNA, eRNA-1 and eRNA-3 transcripts at baseline and after KCl-mediated depolarization. Cell nuclei are stained with DAPI (blue), RNA transcripts are marked by smFISH probes (red). Scale bar 2 μm. **D**, Quantification of spot detection using StarSearch. Number of detected spots for *Fos* mRNA and *Fos* eRNA-1 changes significantly after stimulation (Mann-Whitney test for *Gapdh* n(veh)20, n(KCl)=13, U=116, p>0.05; *Fos* mRNA n(veh)=41, n(KCl)=66, U=237, p<0.0001; eRNA-1 n(Veh)=64, n(KCl)=72, U=1627, p>0.001; eRNA-3 n(veh)=32, n(KCl)=27, U=316.5, p>0.05). Data expressed as mean ± s.e.m. Multiple comparisons, *p<0.05, **p<0.01, ***p<0.001, ****p<0.0001.

responsible for synthesis of *Fos* eRNA, we next performed chromatin immunoprecipitation (ChIP) for RNAP2 following KCl depolarization. KCl-induced *Fos* eRNA transcription is associated with significant recruitment (roughly 2-fold increase) of RNAP2 at the *Fos* enhancer-1 locus, as well as an expected increase at the *Fos* gene promoter (**Fig. 2C**). Moreover, pre-treatment with 5,6-dichloro-1-β-D-ribofuranosylbenzimidazole (DRB; a potent inhibitor of RNAP2-dependent transcription) prior to incubation with KCl resulted in significant blockade of KCl-induced expression of both *Fos* eRNA-1 and *Fos* mRNA (**Fig. 2D**). These results confirm that activity-dependent expression of *Fos* eRNA-1 is associated with RNAP2 recruitment and is dependent on RNAP2 activity for synthesis.

smFISH confirms activity dependence and nuclear localization of eRNAs

To gain insight into the spatial distribution of eRNAs and their response to stimulation, we performed single molecule fluorescent *in situ* hybridization (smFISH), a technique that allows visualization of individual eRNA and mRNA transcripts on a single cell level. Using this tool, we investigated whether the number or localization of our RNA transcripts of interest changed in response to neuronal activation. Cells were KCl-treated for 1 hr prior to fixation, permeabilization, and hybridization with fluorescent smFISH probes. We designed custom probe sets to selectively target and mark individual *Gapdh* and *Fos* mRNA, as well as *Fos* eRNA transcripts arising from two enhancers (enhancer-1 and -3) upstream and downstream of the *Fos* gene (**Fig. 3A**). Punctae indicating eRNA transcripts were almost exclusively restricted to the nucleus whereas

mRNA transcripts were detected in both the cytosol and nucleus (**Fig. 3B**). As shown in **Figure 3C-D**, the number of *Gapdh* transcripts was unaffected by neuronal depolarization while, as expected, the level of *Fos* mRNA signal increased in KCl-treated cells. Interestingly, we detected only a few, but very discrete puncta per cell with both eRNA probe sets (*Fos* eRNA-1 and -3). Larger high-intensity foci are typically associated with active transcription sites as they indicate an accumulation of transcripts. We observed this phenomenon frequently in the quantification of *Fos* mRNA signal, where active transcription is expected in response to depolarization. However, for eRNAs we found such high-intensity puncta to occur much more frequently in both treatment groups, suggesting an accumulation of transcripts at these sites. If these bright punctae were true transcription sites, we would expect to detect up to two loci per nucleus. Surprisingly, both eRNAs intermittently displayed more than two transcript accumulation sites, indicating that eRNAs concentrate and potentially act at several specific loci within the nucleus.

In agreement with our RT-qPCR data (**Fig. 2A**), we detected significantly more *Fos* eRNA-1 puncta after KCl treatment compared to the vehicle group. Unexpectedly, we detected no change in *Fos* eRNA-3 punctae after KCl stimulation, despite the fact that Poly-A- RNA seq (**Fig. 1**) revealed a KCl-induced increase in non-PolyA RNA reads that map to the *Fos* enhancer-3 region. Given that *Gapdh* signal was consistent in both treatment groups, it is unlikely that KCl-treatment itself could affect or impair the eRNA-3 signal. One possible explanation is that *Fos* eRNA-3 transcripts are recruited to only a few distinct sites. KCl induced eRNA-3 transcripts could accumulate at the same target locations resulting in the same number of detected foci despite increased expression.

Enhancer RNAs are sufficient to promote mRNA expression

Active enhancers can be identified by their characteristic epigenetic marks as well as bidirectional transcription (Bose et al., 2017; Li et al., 2016). Therefore, we decided to investigate whether the recruitment of transcriptional activators can activate individual enhancers and whether this affects expression of local eRNAs and linked mRNAs. We employed CRISPRa, a technique that allows anchoring of transcriptional activators (such as VPR or VP64) to different genomic target sites. We designed CRISPR guide RNAs (gRNAs) to target our CRISPRa system to two enhancers sites

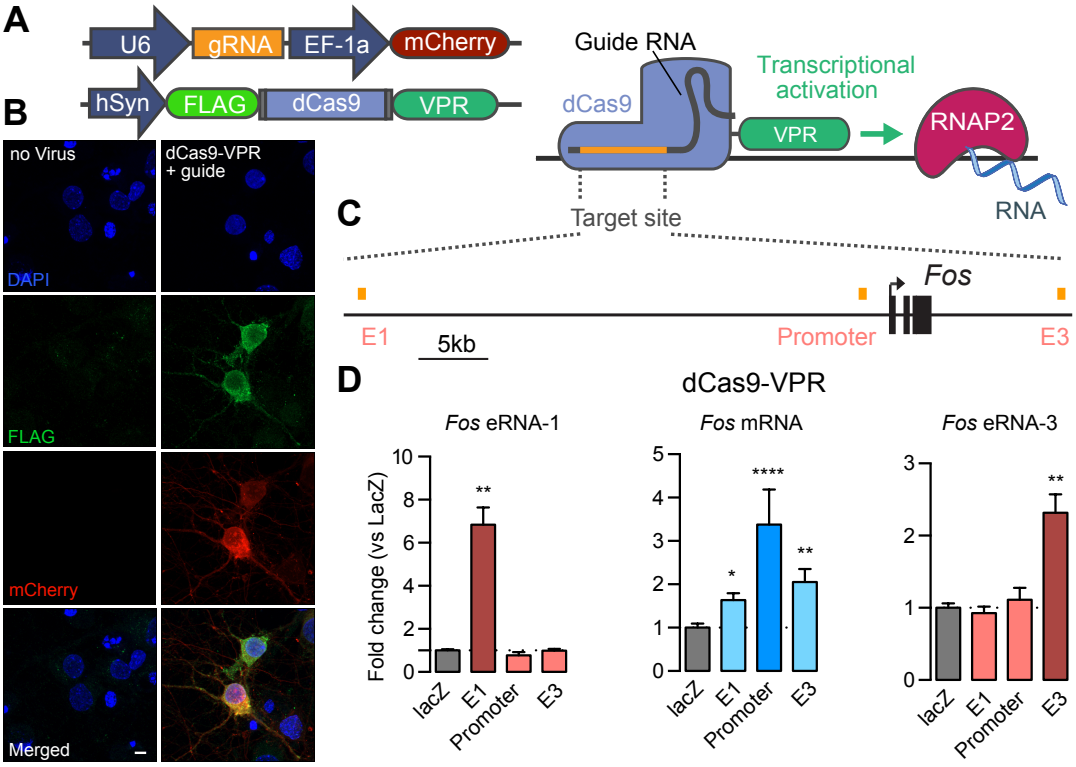

Figure 4. Enhancer activation increases *Fos* eRNA and mRNA expression. **A**, Illustration of CRISPR activation (CRISPRa) strategy for site-specific targeting of the transcriptional activator VPR. **B**, IHC on DIV11 neurons. Left, no virus control. Right, neurons transduced with VPR containing lentivirus (dCas-VPR expression marked by FLAG, gRNA expression marked by mCherry reporter, Scale bar 5 μm). **C**, Target sites of gRNAs at 2 *Fos* enhancers, and one *Fos* promoter site. **D**, RT-qPCR analysis of VPR mediated induction of Fos eRNAs and mRNA when targeted to individual sites surrounding the Fos gene, compared to the non-targeting lacZ control. CRISPRa resulted in site-specific upregulation of selected eRNAs and mRNA. Increasing *Fos* eRNA-1 and eRNA-3 levels resulted in increased *Fos* mRNA levels but not vice versa (n=9 per group; one-way ANOVA for eRNA-1 ($F(4,48)=30.34$, $p<0.0001$), eRNA-3 ($F(4,48)=18.33$, $p<0.001$), and mRNA ($F(4,48)=20.13$, $p<0.001$); Dunnett's multiple comparisons test). Data expressed as mean ± s.e.m. Multiple comparisons, *p<0.05, **p<0.01, ***p<0.001, ****p<0.0001.

surrounding the *Fos* gene, as well as one gRNA targeting the *Fos* promoter to drive mRNA expression directly **(Fig. 4, Fig. S1)**. In addition, we constructed a guide for *LacZ*, a bacterial gene that is not present in eukaryotes, as a non-targeting control.

On DIV4 cortical cultured neurons were transduced with lentiviruses containing VPR and guide construct. After a 7 day incubation period we confirmed plasmid expression (indicated by mCherry reporter for gRNA constructs and FLAG for the VPR construct) and extracted RNA for RT-qPCR. As shown in **Figure 4D**, VPR significantly induced expression of eRNAs from both of the targeted enhancers (enhancer-1 and enhancer-3) when compared to the *LacZ* control. Likewise, targeting the *Fos* promoter resulted in increased *Fos* mRNA levels. Activation of enhancer-1 or enhancer-3, accompanied by local eRNA induction, significantly increased *Fos* mRNA expression. This strongly indicates that enhancers and eRNAs can be induced by transcriptional activators.

In agreement with our neuronal culture data we found that in C6 cells, a rat glial tumor cell line that is more easily manipulated than primary neurons, both tested transcriptional activators (VPR and VP64) induced transcription at the *Fos* promoter and enhancers. Activation of enhancer-1 or enhancer-3 also significantly increased *Fos* mRNA expression (**Fig. S1D-E)**. In addition to this, we observed similar results with enhancer-based epigenetic modifications, as recruitment of dCas9-p300 (a histone acetyltransferase and transcriptional co-activator) to *Fos* E1 induced *Fos* eRNA-1 transcription and elevated *Fos* mRNA (**Fig. S2**). Given that enhancers can interact with promoters it is possible that, in enhancer-promoter loops, transcriptional activators are close enough to act simultaneously on enhancers and promoters. However, we observed no effect on *Fos* eRNA expression when we targeted the promoter to drive mRNA expression (**Fig. 4D, Fig. S1D-E)**, which supports the site-specificity of the observed CRISPRa effects. Overall, these findings imply that enhancers can be activated in a site-specific manner and that the observed increases in *Fos* mRNA are in fact the result of enhancer activation and potentially increased eRNA levels.

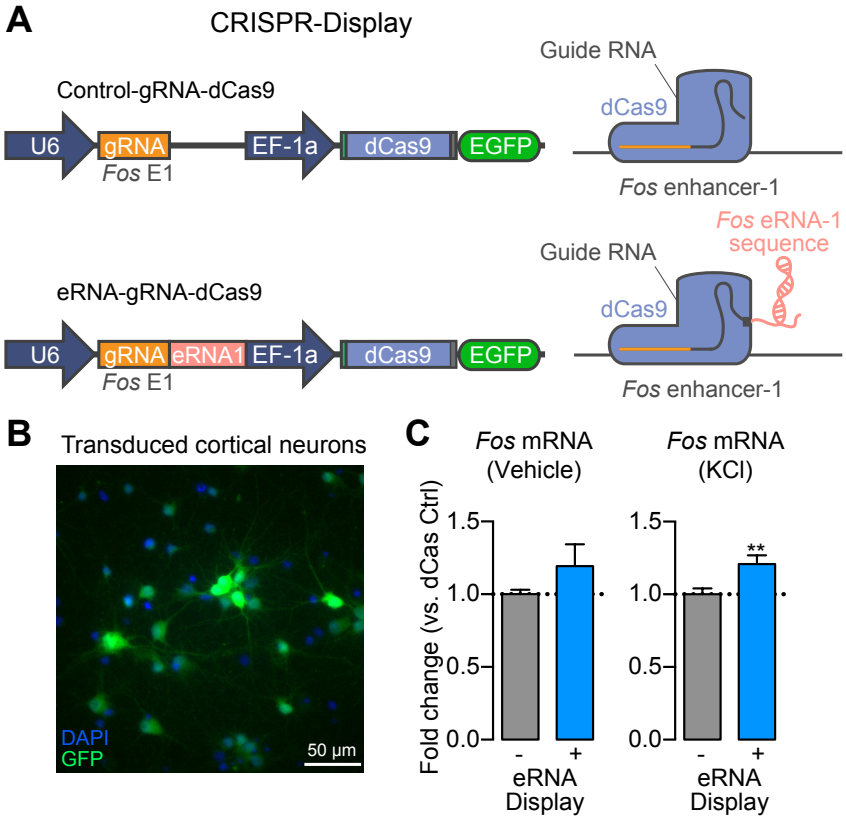

Figure 5. *Fos* eRNA-1 is necessary for *Fos* mRNA expression in neurons. **A**, Illustration of CRISPR-Display strategy for *Fos* eRNA localization to *Fos* enhancer-1. *Fos* eRNA-1 sequence was expressed with specific guide RNAs to target selected enhancers. **B**, Cultured cortical neurons transduced with lentivirus containing *Fos* eRNA-1 CRISPR-Display construct. Neurons were transduced at 4DIV and IHC with anti-GFP antibodies was performed at 11DIV. **C**, RT-qPCR analysis reveals that targeting eRNA-1 to enhancer-1 results in stronger *Fos* mRNA induction upon activation, but not at baseline (n=9 per group, Mann-Whitney test Baseline U=28, p=0.29, and Activation U=11.50, p<0.01). Data expressed as mean ± s.e.m. Multiple comparisons, *p<0.05, **p<0.01, ***p<0.001, ****p<0.0001.

Considering that the mechanisms by which eRNA can regulate proximal mRNA transcription is widely unknown, we explored the effect of localized eRNAs on the expression of linked genes. To do so, we employed CRISPR-Display (Shechner et al., 2015), a novel CRISPR approach that allowed us to tether a specific eRNA sequence to chosen target sites in the genome and investigate local effects, as compared to global over-expression approaches. Given that induction of eRNAs from *Fos* enhancer-1 showed robust effects on mRNA expression in neurons as well as in C6 cells, we designed the Display accessory-RNA sequence based on a conserved region within that particular enhancer element (**Fig. 5A, Fig. S3**). We packaged the

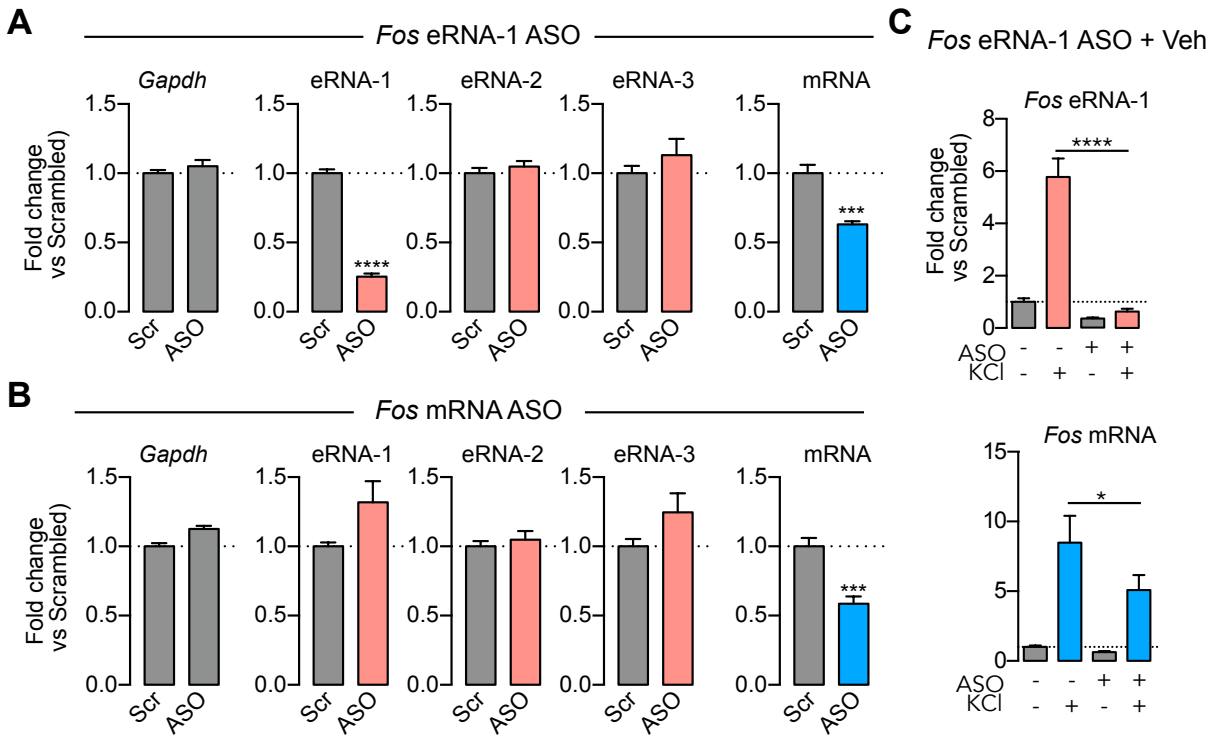

Figure 6. *Fos* eRNA-1 is necessary for *Fos* mRNA expression in neurons. **A**, Anti-sense oligonucleotide (ASO) targeting of *Fos* eRNA-1 for 24h decreased both eRNA-1 and *Fos* mRNA (unpaired t-test t(10)=20.69, p<0.0001 and t(10)=5.739, p<0.001), but did not alter eRNA levels from other *Fos* enhancers. **B**, *Fos* mRNA targeting ASOs decreased mRNA (t(10)=5.198, p<0.001) with no significant effect on eRNA levels. **C**, 24h *Fos* eRNA-1 ASO pretreatment prior to 1h KCl stimulation reduced induction of eRNA-1 (top) and mRNA (bottom) in response to depolarization when compared to a scrambled ASO control (unpaired t-tests, Veh eRNA-1: t(16)=4.332, p=0.0005; Veh mRNA: t(16)=2.454, p=0.0295; KCl eRNA-1: t(16)=17.12, p<0.0001; KCl mRNA: t(16)=3.772, p=0.0017).. Data expressed as mean ± s.e.m. Multiple comparisons, *p<0.05, **p<0.01, ***p<0.001, ****p<0.0001.

construct into a lentivirus and transduced primary rat cortical neuronal cultures with *Fos* enhancer-1 targeting control virus or virus expressing the eRNA-tethering Display construct on DIV 4 **(Fig. 5B-C)**. Following a 7 day incubation period to allow for sufficient viral expression, cells underwent a 1 hr vehicle or KCl treatment prior to RNA extraction and RT-qPCR on DIV 11. Anchoring of this eRNA-1 based sequence in close proximity to enhancer-1 resulted in stronger *Fos* mRNA induction in response to KCl-mediated neuronal depolarization (**Fig. 5C**). The same eRNA-tethering CRISPR-Display construct also achieved an increase in *Fos* mRNA expression at baseline in nucleofected C6 cells **(Fig. S3)**. Taken together, these results support a model in which eRNAs act locally on a genomic region to facilitate transcriptional induction. More importantly, these experiments provide novel evidence that *Fos* eRNA-1 is sufficient to induce the *Fos* gene and enhance mRNA transcription in response to a stimulus.

Enhancer RNAs are necessary for induction of mRNA

A number of reports suggest that eRNAs are induced prior to downstream mRNA activation, and that eRNA synthesis from enhancers is strongly linked to their activity and looping capability (Arner et al., 2015; Li et al., 2013; Li et al., 2016; Sanyal et al., 2012). However, the functional role of these transcripts has remained controversial. To further interrogate the functional role of eRNAs in activity-dependent gene transcription in cortical neurons, we employed an anti-sense oligonucleotide (ASO) strategy to directly target eRNAs while leaving mRNA and other enhancer functions unperturbed. We designed ASOs that target specific sequences of the *Fos* eRNA-1, the eRNA transcript that is most distal to the *Fos* gene. Rat primary cortical cultures were treated with sequence-specific eRNA-1 ASOs for 24 hrs prior to RNA harvesting followed by RT-qPCR (**Fig. 6A**). ASOs targeted to *Fos* eRNA-1 induced a robust decrease in eRNA-1 expression, but did not alter expression of eRNAs from other *Fos* gene enhancers (again suggestive of functional independence of *Fos* eRNAs). Notably, *Fos* eRNA-1 ASOs also produced a significant decrease in *Fos* mRNA levels, both at baseline and following neuronal depolarization with KCl (**Fig. 6A-**

C). These results suggest that *Fos* eRNA-1 is required for normal expression from the *Fos* gene, and that eRNA-1 is required for neuronal activation to induce expression of this immediate early gene. In contrast, we found that knockdown of *Fos* mRNA with a distinct targeted ASO had no effect on eRNA synthesis from any enhancer (**Fig. 6B**), demonstrating a unidirectional relationship between eRNA and mRNA function.

Enhancer RNAs are necessary for neuronal firing at baseline and in response to activation

Enhancers have been demonstrated to be fundamental regulators of activity- and experience-dependent gene expression in the context of neuronal plasticity and memory formation (Joo et al., 2016; Kim et al., 2010; Malik et al., 2014; Schaukowitch et al., 2014; Telese et al., 2015) in agreement with our data that indicate that eRNAs are crucial regulators of activity-dependent gene transcription in cortical neurons. However, if and how active enhancers or even a single eRNA affect electrophysiological properties of neurons remains an open question. To investigate the significance of individual eRNAs in neuronal activity, we utilized multielectrode arrays (MEAs) to record neuronal activity in response to decreased (ASOs) *Fos* eRNA-1 levels. Rat primary cortical cultures grown on MEAs were treated with sequence-specific eRNA-1 ASOs or a scrambled control ASO for 24 hrs. Notably, firing patterns did not differ between wells prior to ASO treatment (Data not shown). Electrophysiological recordings were carried out for 20 min to establish a stable baseline, followed by a 10-min recording during which gabazine (GBZ), a $GABA_A$ antagonist, was added **(Fig. 7A)**. ASO-mediated knock down of *Fos* eRNA-1 resulted in a robust decrease in action potential frequency (**Fig. 7D, F**) and number of action potential bursts at baseline as well as in response to neuronal activity (**Fig. 7E, G**). Intriguingly, we observed that by decreasing eRNA-1 we were able to block gabazine-induced changes in firing rates completely (**Fig. 7D**). Overall, these findings demonstrate that altering the levels of a single eRNA is sufficient to modulate firing patterns, highlighting the importance of eRNAs not only in gene expression but also in neuronal function.

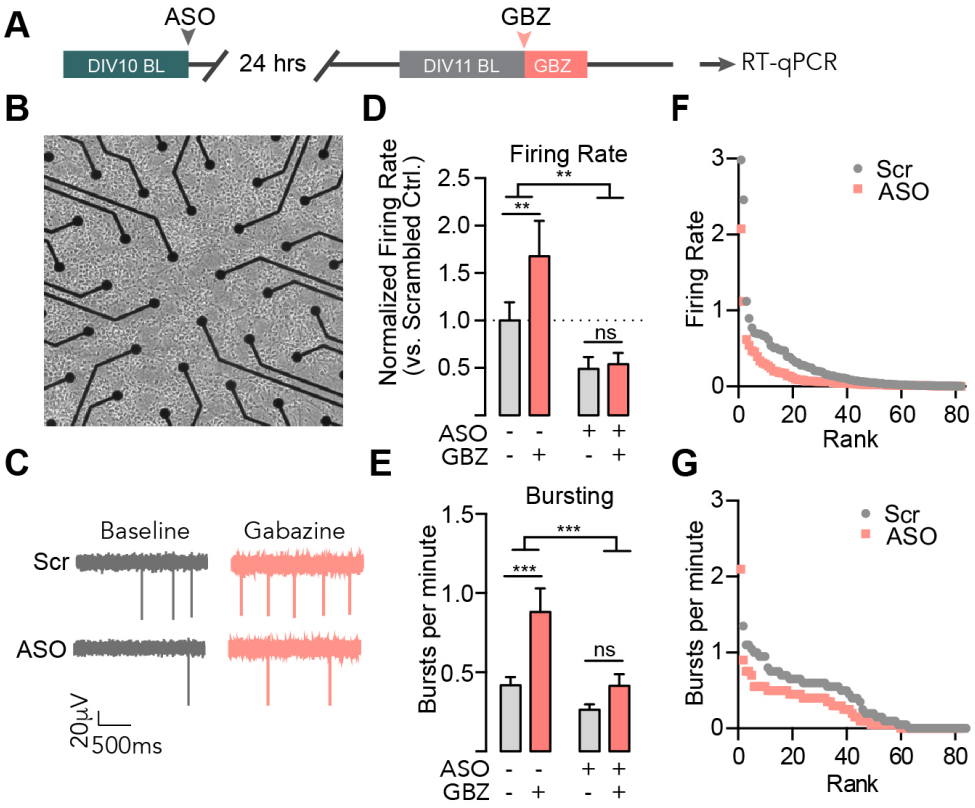

Figure 7. *Fos* eRNA-1 is necessary for normal neuronal activity at baseline and in response to activation. **A**, Timeline of recordings (boxes) and treatments (arrows). **B,** Primary neuronal cortex cultures grown on a multi electrode array (MEA) plate. **C**, Example traces of scrambled or eRNA1 targeting ASO treated neurons at baseline and in response to treatment with 5μM gabazine. **D-E,** ASO mediated decreases in *Fos* eRNA-1 levels result in lower firing rates at baseline, fewer bursts per minute, and prevent the response to gabazine treatment. **F-G,** Ranked baseline firing rates and bursts per minute after scrambled ASO or eRNA-1 targeting ASO treatment indicate stronger ASO effects in highly active neurons. Data expressed as mean ± s.e.m. Multiple comparisons, *p<0.05, **p<0.01, ***p<0.001, ****p<0.0001.

Discussion

Distal enhancer elements in DNA enable higher-order chromatin interactions that facilitate gene expression programs and thus contribute to cellular phenotype and function (Heinz et al., 2015; Li et al., 2016; Wang et al., 2011). In the developing brain, the majority of enhancer elements exhibit temporally specific emergence during precise

developmental windows, with only ~15% of enhancers being utilized continually from late embryonic development into adulthood (Gray et al., 2015; Nord et al., 2013). These developmentally regulated enhancers contribute to cell- and tissue-specific gene expression patterns that establish communication within and between brain structures (Frank et al., 2015; Nord et al., 2013; Pattabiraman et al., 2014). Not surprisingly, enhancers utilized in early embryonic brain development possess the highest degree of sequence conservation across species, suggesting that robust evolutionary pressures drive enhancer function (Nord et al., 2013). In the postnatal and mature brain, enhancers continue to play a widespread role in the activity-dependent transcriptional programs that regulate key aspects of neuronal plasticity and function (Gray et al., 2015; Hnisz et al., 2013; Joo et al., 2016; Kim et al., 2010; Malik et al., 2014; Telese et al., 2015; Vermunt et al., 2014). Repression or deletion of enhancer elements has profound effects on the genes that they control, including complete inactivation (Joo et al., 2016; Kearns et al., 2015; Malik et al., 2014; Telese et al., 2015). Likewise, targeted enhancer activation induces robust upregulation of linked genes, suggesting that enhancers serve as bidirectional regulators of gene activity (Frank et al., 2015; Hilton et al., 2015).

Although it is well accepted that genomic enhancers play critical roles in tuning the spatiotemporal nature of transcription from linked genes, techniques typically used to examine enhancer function (e.g., enhancer deletion (Leighton et al., 1995), Cas9-based mutation (Lopes et al., 2016; Sanjana et al., 2016), or activation/inactivation with dCas9 fusion proteins (Hilton et al., 2015; Joo et al., 2016; Liu et al., 2017; Liu et al., 2016)) interfere with both the genomic locus and eRNAs transcribed from that locus. Therefore, these approaches cannot dissociate the effects of enhancer function and eRNA function. To address this problem we took two different approaches that directly target eRNAs in order to examine their function separately from enhancer function. First, we used a novel CRISPR-Display approach in neuronal cultures to target *Fos* eRNA to its own enhancer. These results demonstrate that *Fos* eRNA is sufficient to induce *Fos* mRNA. Secondly, we employed stable, cell-penetrating ASOs to target eRNA for degradation. These results suggest that eRNA is necessary for normal expression of *Fos* mRNA, both under basal conditions and after neuronal depolarization. Finally, our results show that altered levels of a single eRNA without any changes to the underlying enhancer sequence is sufficient to modulate neuronal firing patterns (**Fig. 7**). Together, these findings strongly support a critical role for eRNAs in regulation of gene expression programs induced in response to neuronal activation.

Overall, these results are in agreement with a previous report demonstrating that eRNAs transcribed from activity-dependent enhancers are necessary for induction of mRNA from linked genes (Schaukowitch et al., 2014). This report utilized lentiviral shRNA knockdown approaches to directly target activity-induced eRNAs near *Arc* and *Gadd45b* genes, and followed this knockdown with KCl depolarization to induce mRNAs. Targeted shRNA knockdown of eRNA specifically blocked mRNA induction at these genes, but not other IEGs induced by neuronal activation (*Fos*, *Egr1*). Our results extend these important findings in two ways. First, given that the *Fos* gene exhibits multiple enhancers and activity-dependent eRNAs, we were able to address the functional relationship between eRNAs near the same gene. Our results suggest that while eRNAs do regulate mRNA induction at linked genes, eRNAs are functionally independent of each other. Thus, ASO-mediated knockdown of eRNAs transcribed from the most distal *Fos* enhancer did not downregulate eRNAs transcribed from other enhancers (**Fig. 6**). Secondly, in parallel experiments we were able to target *Fos* mRNA for knockdown using an identical approach. These results demonstrate that the relationship between eRNA and mRNA levels at the same gene is unidirectional – i.e., that mRNA knockdown does not also reduce eRNA levels. This is a critical control at IEGs like *Fos*, given that the protein product of this gene is a transcription factor that localizes to enhancers in an AP1 complex with Jun family members (Malik et al., 2014).

Biological roles of lncRNAs are generally linked to their ability to bind functionally active proteins to operate as molecular guides, decoy molecules, scaffolding, or even allosteric modulators (Quinn and Chang, 2016; Rinn and Chang, 2012). In agreement with this concept, a large number of chromatin associated proteins bind RNA in addition to DNA (Di Ruscio et al., 2013; Hendrickson et al., 2016; Savell et al., 2016), and several well-characterized transcriptional

regulators have recently been shown to possess functional interactions with eRNAs (Bose et al., 2017; Hsieh et al., 2014; Lai et al., 2013; Li et al., 2013; Li et al., 2016; Schaukowitch et al., 2014; Sigova et al., 2015). For example, eRNAs interact with CREB binding protein (CBP) and stimulate its activity as a histone acetyltransferase at enhancer loci (Bose et al., 2017). Likewise, eRNAs have been shown to bind the ubiquitous transcription factor Yin-Yang 1 (YY1) to "trap" YY1 at the enhancer, thus facilitating its action at local YY1 motifs in DNA (Sigova et al., 2015). Finally, eRNAs can act as decoy molecules for negative elongation factor (NELF) complexes, which are important regulators of RNAP2 pausing and transcriptional bursting (Schaukowitch et al., 2014). While our results do not reveal how eRNA-protein interactions may direct enhancer functions in neurons, our results add to this existing evidence by showing that eRNAs transcribed from a single enhancer can exist at multiple locations in a nucleus and, when targeted to a specific enhancer using CRISPR-Display, are sufficient to regulate expression of linked genes.

The vast majority of gene variants linked to human health and disease by genome-wide association studies are located in non-coding regions of the genome (Gordon and Lyonnet, 2014; Network and Pathway Analysis Subgroup of Psychiatric Genomics, 2015; Schizophrenia Working Group of the Psychiatric Genomics, 2014; Vermunt et al., 2014), with putative enhancers containing more disease-linked single-nucleotide polymorphisms than all other genetic loci combined (Corradin and Scacheri, 2014). Disease-linked genetic variants could affect enhancer activity either via direct modification of enhancer DNA sequence (e.g., disruption of a transcription factor motif), or by alterations in long-range chromatin interactions between enhancers and gene promoters. Indeed, numerous diseases have already been linked to sequence variations in enhancer regions (Gordon and Lyonnet, 2014; Jeong et al., 2008; Spieler et al., 2014; Vermunt et al., 2014), including complex polygenic conditions such as depression (Davidson et al., 2011; Edwards et al., 2012), obesity (Davidson et al., 2011; Voisin et al., 2015), schizophrenia (Eckart et al., 2016; Roussos et al., 2014), bipolar disorder (Eckart et al., 2016), and autism spectrum disorders (Inoue and Inoue, 2016; Yao et al., 2015). This growing link between enhancer activity and brain function strongly highlights the need to better understand the mechanistic interactions that regulate enhancer function at the molecular level, and also suggests that enhancers could be attractive targets for a new generation of disease therapeutics.

Methods

Genome-wide quantification and characterization of eRNA species. Identification and characterization of transcriptionally active enhancers was performed using previously published non-PolyA RNA-seq datasets (available under GEO accession number GSE64988) (Savell et al., 2016). This dataset was generated using rat DIV 11 cortical neuron cultures treated for 1 hr with vehicle, 25 mM KCl, or 1 μM TTX. Extracted RNA underwent two selection processes. First, polyadenylated (PolyA+) RNA was captured with the NEBNext Poly(A) mRNA Magnetic Isolation Module. Secondly, the remaining non-polyadenylated (non-PolyA) underwent ribosomal RNA depletion (NEBNext rRNA depletion kit) prior to directional, 50bp, paired-end sequencing on an Illumina HiSeq 2000 platform. Raw paired-end sequenced reads were quality controlled, filtered for read quality (FASTX toolkit, Galaxy) and aligned to the rat Rn5 genome sequence in Galaxy using Tophat v1.4.0. General analyses were performed in Seqmonk v1.38.2 (Babraham Institute), using a merged dataset of ~118 million mapped non-PolyA reads from six independent biological replicates (two per treatment group).

For genome-wide characterization of transcriptionally active enhancer elements and enhancer identification, we used an RNA-driven pipeline. Genome-aligned BAM files were probed for contiguously transcribed elements (>100bp, merging elements closer than 1kb) using reads on both strands. Using a 12x read depth cutoff, we identified 31,346 regions of contiguous transcription, of which 18,422 fell within 1kb or overlapped annotated genes. Due to the difficulty in separating intronic enhancers from potential promoters or other elements, these were removed from consideration. The 12,924 regions remaining were designated as transcribed intergenic regions (TIRs). Next, to capture TIRs that corresponded to enhancers, we filtered this list against overlapping histone modification peaks from adult mouse cortex (ENCODE project datasets obtained from the UCSC Table Browser and transformed from mm9

to Rn5 genome coordinates using Liftover). Of 12,924 TIRs, 22.5% overlapped H3K4me1 peaks, a mark commonly used to denote active enhancers. Likewise, an additional 5.2% of TIRs overlapped adult cortex H3K4me3 and H3K27ac, which are commonly used to mark poised enhancers. Together, this combination of 3,107 transcriptionally active enhancers (TAEs) was characterized for other key elements, including RNAP2 and CTCF binding (ENCODE project datasets obtained from the UCSC Table Browser and transformed from mm9 to Rn5 genome coordinates using Liftover), and sequence conservation (PhastCons13way species conserved element BED file) or CpG islands (both obtained from UCSC Table Browser using Rn5 genome coordinates).

For differential comparison of eRNA elements that are altered by neuronal depolarization (termed activity-responsive TAEs, or arTAEs), we quantified and compared read counts in Vehicle and KCl non-PolyA RNA-seq libraries at all 3,107 transcriptionally active enhancers using DESeq2 (Seqmonk wrapper for R; corrected for multiple comparisons, FDR = 0.05). Of 3,107 enhancer elements, 89 exhibited significant differential regulation by KCl depolarization. For quantification of mRNA transcripts at nearby genes, PolyA+ datasets from the same experiments were used to compute log2(fold change) for differentially expressed genes (230 differentially expressed genes identified using DESeq2, corrected for multiple comparisons, FDR = 0.05).

Cultured neuron experiments. Primary rat cortical neuronal cultures were generated from embryonic day 18 rat cortical tissue as described previously (Day et al., 2013; Savell et al., 2016). Briefly, cell culture wells and MEAs were coated overnight at 37° C with poly-L-lysine (50 µg/ml) and rinsed with diH_2O. Dissected cortices were incubated with papain for 25 min at 37°C. After rinsing in Hank's Balanced Salt Solution (HBSS), a single cell suspension of the tissue was re-suspended in Neurobasal media (Invitrogen) by trituration through a series of large to small fire-polished Pasteur pipets. Primary neuronal cells passed through a 70 μM cell strainer were plated on poly-lysine coated culture wells. Cells were spun and re-suspended in fresh media, counted, and plated to a density of 100,000 cells per well on 6-well MEA plates, and 250,000 cells per well on 12-well culture plate with or without glass coverslips (60,000 cells/cm). Cells were grown in Neurobasal media plus B-27 and L-glutamine supplement (complete Neurobasal media) for 11 days in vitro in a humidified CO_2 (5%) incubator at 37° C. MEAs were switched to BrainPhys media (Stemcell Technologies Inc.) plus SM1 and L-glutamine supplement on DIV5.

At 4-11 days in vitro, neuronal cultures were treated as described. For KCl stimulation experiments, KCl (Sigma) was added to complete Neurobasal media (2X specified concentration), and half of the cell culture media (500 μl) was replaced with KCl solution or vehicle (complete Neurobasal media alone).

Cells were incubated with KCl for described time points prior to RNA extraction. For TTX inactivation experiments, cells were treated with 1 μM TTX (Tocris Bioscience) in Neurobasal media for the described time points prior to RNA extraction. S-AMPA, NMDA, and Forskolin (Sigma) were diluted in sterile water and added to cultures for 1 hr at a volume of 10 μl (final concentrations of 1 μM, 10 μM, or 100 μM). 10 μl sterile water was added as a vehicle control. For experiments involving RNAP inhibitors, cultures were treated for 4 hrs or 4 hrs followed by a 1 hr, 25 mM KCl stimulation. The RNAP2-dependent transcriptional inhibitor DRB (Sigma) was dissolved to a 20 mM stock solution in 100% cell culture grade DMSO (Sigma) and diluted in Neurobasal media to described experimental concentrations. Vehicle treated cells received equal concentrations of DMSO in Neurobasal media. At a minimum, all cell culture experiments were performed in triplicate.
For viral transduction cells were transduced with 5 µl plasmid containing virus on DIV 4 (minimum $3.97x10^8$ IU/ml for a final MOI of 7.94). After a 24 hrs incubation period virus containing media was replaced with conditioned media from an untreated control plate to minimize toxicity. A regular half media change followed on DIV 8. On DIV 11 transduced cells were imaged and virus expression was verified prior to KCl-treatment and RNA extraction. IHC for GFP protein was performed as described previously (Savell et al., 2016), with a monoclonal anti-GFP antibody (MAB3580, Millipore, RRID:AB_94936).

RNA extraction and RT-qPCR. Total RNA was extracted (RNAeasy kit, Qiagen) with DNase

treatment (RNase free DNAse, Qiagen), and reverse-transcribed (iScript cDNA Synthesis Kit, Bio- Rad). cDNA was subject to RT-PCR for genes of interest, as described previously(Savell et al., 2016). A list of PCR primer sequences is provided in **Supplementary Data Table 3**.

Chromatin immunoprecipitation (ChIP). Following KCl stimulation, neuronal cultures (~3,000,000 million cortical neurons per treatment group) were fixed with 1% paraformaldehyde in 1x PBS plus Halt Inhibitor Cocktail (ThermoFisher) and washed with 1x PBS. Cells were then extracted and lysed in Lysis Buffer (50 mM HEPES, 10 mM NaCl, 1 mM EDTA, 0.5% NP-40, Halt Cocktail), spun down, and resuspended in 100 *µ*l of RIPA Buffer (1% NP-40, 1% SDS, HALT Cocktail in 1x PBS). Following resuspension, each sample was sheared via sonication (BioRuptor Pico) and spun down once again to remove debris. The resulting supernatant was diluted to 1 ml using RIPA buffer and aliquoted into input and IP samples. Immunoprecipitation was performed with a RNAP2 antibody (Active Motif, 39097). Antibody-protein complexes were isolated with magnetic beads (Dynabeads protein A, Invitrogen). Each sample was incubated overnight at 4°C. Following incubation, all samples were washed sequentially with Low-salt immune complex buffer (Millipore), High-salt immune complex buffer (Millipore), LiCl immune complex buffer (Millipore), and Tris-EDTA (TE) buffer (Fisher Scientific). To revert protein-DNA crosslinks, samples were resuspended in TE buffer plus 1% SDS, RNase, and Proteinase K and incubated for 2 hrs at 65°C. The resultant DNA was then purified using a PCR cleanup kit (Qiagen), and levels of protein-DNA interactions were measured using qPCR.

CRISPR-dCas9 construct design. To achieve transcriptional activation, lentivirus-compatible VP64 and VPR constructs were engineered to express dCas, and either transcriptional activator. dCAS9-VP64_GFP was a gift from Feng Zhang (Addgene plasmid # 61422 (Konermann et al., 2015)). SP-dCas9-VPR was a gift from George Church (Addgene plasmid # 63798 (Chavez et al., 2015)), which was edited by insertion of the dCas9-VPR cassette into a lentivirus-compatible backbone. The pcDNA-dCas9-p300 Core construct was a gift from Charles Gersbach (Addgene plasmid # 61357 (Hilton et al., 2015)). VP64 and VPR expressing constructs were co-transfected with gRNA containing constructs. Gene-specific gRNAs were designed using an online gRNA tool, provided by the Zhang Lab at MIT (crispr.mit.edu). To ensure specificity all CRISPR RNAs (crRNAs) were analyzed with BLAST. gRNAs were designed to target all three *Fos* enhancers respectively, as well as the promoter region of *Fos* (a list of the target sequences is provided in **Supplementary Data Table 3**). crRNA was annealed and ligated into the gRNA scaffold using the BsmBI cut site. Plasmids were sequence-verified with Sanger sequencing. For CRISPR-Display, lentiCRISPR v2 from Feng Zhang (Addgene plasmid # 52961 (Sanjana et al., 2014)) was modified, and engineered to express dCas9 (instead of Cas9), gRNA, an 100bp sequence of eRNA-1 and GFP via restriction enzyme cloning using gBlocks for eRNA-1 (cut with SwaI and EcoRI) and GFP (cut with MluI and BamHI) respectively. As a control, a plasmid lacking the eRNA sequence was targeted to the same genomic sites.

C6 Cell Culturing and Nucleofection. C6 cells were obtained from American Type Culture Collection (CCL-107, ATCC, RRID:CVCL_0194) and cultured in F-12k based medium (2.5% bovine serum, 12% horse serum). At each passage, cells were trypsinized for 1-3 min (0.25% trypsin and 1 mM EDTA in PBS pH 7.4) at room temperature. After each passage remaining cells were processed for nucleofection (2 x10^6 /group). Cell pellets were resuspended in LonzaD nucleofection buffer and electroporated with 3.4ug plasmid DNA per group. Nucleofector™2b device (Lonza) was used according to the manufacturer's instruction (C6, high efficiency protocol). Nucleofection groups were diluted with 500 µl media respectively and plated in triplicates in 24-well plates (~ 600 0000 cells/well). Plates underwent a full media change 4-6 hrs after nucleofection, and were imaged and frozen for downstream processing after 16 hrs.

Lentivirus production. Viruses were produced in a sterile environment subject to BSL-2 safety by transfecting HEK-293T cells with specified CRISPR-dCas9 plasmids, the psPAX2 packaging plasmid, and the pCMV-VSV-G envelope plasmid (Addgene 12260 & 8454) with FuGene HD (Promega) for 40 hrs. Viral titer was determined using a qPCR Lentivirus Titration(Titer) Kit (Applied Biological Materials). Viruses were stored in sterile

PBS at -80°C.

Antisense oligonucleotide (ASO) design and treatment. To manipulate *Fos* mRNA or eRNA levels, we designed 20 bp ASOs that targeted distinct transcripts from the *Fos* gene locus (see **Supplementary Data Table 3** for target sequences). ASOs targeting exon 3 of *Fos* mRNA or *Fos* eRNA-1 were synthesized with two chemical modifications: an all phosphorothioate backbone and five 2' O-methyl RNA bases on each end of the oligonucleotide (Integrated DNA Technologies). Primary neuronal cultures were treated with scrambled or *Fos* targeted ASOs (15 µM in buffer EB, for a final concentration of 1.5 µM) and incubated for 24 hrs (basal experiments) or 1 hr neuronal depolarization with 25 mM KCl (or vehicle control). Following ASO treatment, RNA was extracted (Qiagen RNeasy kit) and *Fos* mRNA and eRNA levels were determined using RT-qPCR with custom primers.

Single Molecule RNA FISH

smFISH Probe Design

We designed and ordered Stellaris® FISH probe sets for Gapdh mRNA, cFos eRNA-1, eRNA-3 and mRNA carrying a fluorophore (Quasar® 570 for eRNA-1 probes, Quasar® 670 for eRNA-3 and mRNA probes). We preferred probes of 20-mer oligonucleotides. Multiple probes per set targeting the same RNA molecule were designed for an adequate signal to background ratio and to optimize signal strength. The eRNA-1 set contained 36 probes, the eRNA-3 set 30 probes targeting the each eRNA transcript respectively. The *Fos* mRNA probe set contained 30 probes, and the *Gapdh* probe set contained 42 probes (the target sequences of each probe set are provided in **Supplementary Data Table 3**).

Sample Preparation and Hybridization

Day 1: Primary neuronal cultures (~250,000 neurons per coverslip/well) were KCl or Vehicle treated for 1 hr on DIV 11. After treatment cells were cross-linked with 3.7% formaldehyde (paraformaldehyde in 1X PBS) for 10 min at room temperature (21°C) on a rocking platform. Wells were washed twice with PBS and permeabilized in 70% ethanol for at least 3h at 4°C. Wells were washed in Stellaris® Wash Buffer A with for 5 min at room temperature. Coverslips were transferred to a humidifying chamber and incubated with hybridization buffer (0.5 nM mRNA probe, 0.5 nM eRNA probe) for 14 hrs at 37°C.

Day 2: Coverslips were washed twice in Stellaris® Wash Buffer A for 30 min at 37°C. After a 5 min wash in Stellaris® Wash Buffer B at room temperature, coverslips were mounted using ProLong™ antifade with DAPI for imaging.

Quantification of Expression

A number of freely available programs have been developed to quantify smRNA FISH results. We used StarSearch (http://rajlab.seas.upenn.edu/StarSearch/launch.html), which was developed by Marshall J. Levesque and Arjun Raj at the University of Pennsylvania to automatically count individual RNAs. mRNA and eRNA detection involved two major steps. First, images for each probe set as well as a DAPI image are merged and cells were outlined. Punctae detection was carried out and additional adjustment of thresholds was performed. Same threshold range was used for all images.

Multi Electrode Array Recordings

Neuronal activity in response to decreased (ASOs) eRNA levels was recorded for 20 min on DIV11 at baseline, followed by a 10-min recording with 5 *µ*M Gabazine treatment using a 6-well MEA system (Multi Channel Systems MCS GmbH). For comparison, spontaneous activity was also recorded prior to eRNA1 targeting ASO or scrambled ASO treatment on DIV10. MC Rack software (Multi Channel Systems MCS GmbH) was used for recording and thresholding. Offline Sorter (Plexon) and NeuroExplorer® were used for further sorting and analysis.

Statistical Analysis

Transcriptional differences from PCR experiments were compared with one-way ANOVA with Dunnett's post-hoc tests, or Mann-Whitney test where appropriate. Significance of smFISH data was assessed with Mann-Whitney test. Statistical significance was designated at $\alpha = 0.05$ for all analyses. Statistical and graphical analyses were performed with Graphpad software (Prism). Statistical assumptions (e.g., normality and homogeneity for parametric tests) were formally tested and boxplots were examined.

Author contributions

N.V.N.G, R.C.S, and J.J.D conceived of these

experiments, performed experiments, and wrote the manuscript. J.S.R., K.D.B., A.S., K.E.S., and F.A.S assisted in experiments. N.V.N.G, R.C.S, and J.J.D performed bioinformatics analysis. J.J.D. supervised all work.

Acknowledgements

We acknowledge the Civitan International Research Center Cellular Imaging Facility. This work was supported by NIH grants DA039650 and DA034681 and the UAB Pittman Scholar Program (JJD), DA042514 (K.E.S.), DA041778 (F.A.S.), and the CIRC Emerging Scholar Award (NVNG).

References

Arner, E., Daub, C.O., Vitting-Seerup, K., Andersson, R., Lilje, B., Drablos, F., Lennartsson, A., Ronnerblad, M., Hrydziuszko, O., Vitezic, M., *et al.* (2015). Transcribed enhancers lead waves of coordinated transcription in transitioning mammalian cells. Science *347*, 1010-1014.

Bose, D.A., Donahue, G., Reinberg, D., Shiekhattar, R., Bonasio, R., and Berger, S.L. (2017). RNA Binding to CBP Stimulates Histone Acetylation and Transcription. Cell *168*, 135-149 e122.

Chavez, A., Scheiman, J., Vora, S., Pruitt, B.W., Tuttle, M., E, P.R.I., Lin, S., Kiani, S., Guzman, C.D., Wiegand, D.J., *et al.* (2015). Highly efficient Cas9-mediated transcriptional programming. Nat Methods *12*, 326-328.

Corradin, O., and Scacheri, P.C. (2014). Enhancer variants: evaluating functions in common disease. Genome Med *6*, 85.

Davidson, S., Lear, M., Shanley, L., Hing, B., Baizan-Edge, A., Herwig, A., Quinn, J.P., Breen, G., McGuffin, P., Starkey, A., *et al.* (2011). Differential activity by polymorphic variants of a remote enhancer that supports galanin expression in the hypothalamus and amygdala: implications for obesity, depression and alcoholism. Neuropsychopharmacology *36*, 2211-2221.

Day, J.J., Childs, D., Guzman-Karlsson, M.C., Kibe, M., Moulden, J., Song, E., Tahir, A., and Sweatt, J.D. (2013). DNA methylation regulates associative reward learning. Nat Neurosci *16*, 1445-1452.

Di Ruscio, A., Ebralidze, A.K., Benoukraf, T., Amabile, G., Goff, L.A., Terragni, J., Figueroa, M.E., De Figueiredo Pontes, L.L., Alberich-Jorda, M., Zhang, P., *et al.* (2013). DNMT1-interacting RNAs block gene-specific DNA methylation. Nature *503*, 371-376.

Djebali, S., Davis, C.A., Merkel, A., Dobin, A., Lassmann, T., Mortazavi, A., Tanzer, A., Lagarde, J., Lin, W., Schlesinger, F., *et al.* (2012). Landscape of transcription in human cells. Nature *489*, 101-108.

Eckart, N., Song, Q., Yang, R., Wang, R., Zhu, H., McCallion, A.S., and Avramopoulos, D. (2016). Functional Characterization of Schizophrenia-Associated Variation in CACNA1C. PLoS One *11*, e0157086.

Edwards, A.C., Aliev, F., Bierut, L.J., Bucholz, K.K., Edenberg, H., Hesselbrock, V., Kramer, J., Kuperman, S., Nurnberger, J.I., Jr., Schuckit, M.A., *et al.* (2012). Genome-wide association study of comorbid depressive syndrome and alcohol dependence. Psychiatr Genet *22*, 31-41.

Fleischmann, A., Hvalby, O., Jensen, V., Strekalova, T., Zacher, C., Layer, L.E., Kvello, A., Reschke, M., Spanagel, R., Sprengel, R., *et al.* (2003). Impaired long-term memory and NR2A-type NMDA receptor-dependent synaptic plasticity in mice lacking c-Fos in the CNS. J Neurosci *23*, 9116-9122.

Frank, C.L., Liu, F., Wijayatunge, R., Song, L., Biegler, M.T., Yang, M.G., Vockley, C.M., Safi, A., Gersbach, C.A., Crawford, G.E., *et al.* (2015). Regulation of chromatin accessibility and Zic binding at enhancers in the developing cerebellum. Nat Neurosci *18*, 647-656.

Gordon, C.T., and Lyonnet, S. (2014). Enhancer mutations and phenotype modularity. Nat Genet *46*, 3-4.

Gray, J.M., Kim, T.K., West, A.E., Nord, A.S., Markenscoff-Papadimitriou, E., and Lomvardas, S. (2015). Genomic Views of Transcriptional Enhancers: Essential Determinants of Cellular Identity and Activity-Dependent Responses in the CNS. J Neurosci *35*, 13819-13826.

Hangauer, M.J., Vaughn, I.W., and McManus, M.T. (2013). Pervasive transcription of the human genome produces thousands of previously unidentified long intergenic noncoding RNAs. PLoS Genet *9*, e1003569.

Heinz, S., Romanoski, C.E., Benner, C., and Glass, C.K. (2015). The selection and function of cell type-specific enhancers. Nat Rev Mol Cell Biol *16*, 144-154.

Hendrickson, D., Kelley, D.R., Tenen, D., Bernstein, B., and Rinn, J.L. (2016). Widespread RNA binding by chromatin-associated proteins. Genome Biol *17*, 28.

Hilton, I.B., D'Ippolito, A.M., Vockley, C.M., Thakore, P.I., Crawford, G.E., Reddy, T.E., and Gersbach, C.A. (2015). Epigenome editing by a CRISPR-Cas9-based acetyltransferase activates genes from promoters and enhancers. Nat Biotechnol *33*, 510-517.

Hnisz, D., Abraham, B.J., Lee, T.I., Lau, A., Saint-Andre, V., Sigova, A.A., Hoke, H.A., and Young, R.A. (2013). Super-enhancers in the control of cell identity and disease. Cell *155*, 934-947.

Hsieh, C.L., Fei, T., Chen, Y., Li, T., Gao, Y., Wang, X., Sun, T., Sweeney, C.J., Lee, G.S., Chen, S., *et al.* (2014). Enhancer RNAs participate in androgen

receptor-driven looping that selectively enhances gene activation. Proc Natl Acad Sci U S A *111*, 7319-7324.

Inoue, Y.U., and Inoue, T. (2016). Brain enhancer activities at the gene-poor 5p14.1 autism-associated locus. Sci Rep *6*, 31227.

Jeong, Y., Leskow, F.C., El-Jaick, K., Roessler, E., Muenke, M., Yocum, A., Dubourg, C., Li, X., Geng, X., Oliver, G.*, et al.* (2008). Regulation of a remote Shh forebrain enhancer by the Six3 homeoprotein. Nat Genet *40*, 1348-1353.

Joo, J.Y., Schaukowitch, K., Farbiak, L., Kilaru, G., and Kim, T.K. (2016). Stimulus-specific combinatorial functionality of neuronal c-fos enhancers. Nat Neurosci *19*, 75-83.

Kaikkonen, M.U., Spann, N.J., Heinz, S., Romanoski, C.E., Allison, K.A., Stender, J.D., Chun, H.B., Tough, D.F., Prinjha, R.K., Benner, C.*, et al.* (2013). Remodeling of the enhancer landscape during macrophage activation is coupled to enhancer transcription. Mol Cell *51*, 310-325.

Kearns, N.A., Pham, H., Tabak, B., Genga, R.M., Silverstein, N.J., Garber, M., and Maehr, R. (2015). Functional annotation of native enhancers with a Cas9-histone demethylase fusion. Nat Methods *12*, 401-403.

Kim, T.K., Hemberg, M., and Gray, J.M. (2015). Enhancer RNAs: a class of long noncoding RNAs synthesized at enhancers. Cold Spring Harb Perspect Biol *7*, a018622.

Kim, T.K., Hemberg, M., Gray, J.M., Costa, A.M., Bear, D.M., Wu, J., Harmin, D.A., Laptewicz, M., Barbara-Haley, K., Kuersten, S.*, et al.* (2010). Widespread transcription at neuronal activity-regulated enhancers. Nature *465*, 182-187.

Kim, T.K., and Shiekhattar, R. (2015). Architectural and Functional Commonalities between Enhancers and Promoters. Cell *162*, 948-959.

Konermann, S., Brigham, M.D., Trevino, A.E., Joung, J., Abudayyeh, O.O., Barcena, C., Hsu, P.D., Habib, N., Gootenberg, J.S., Nishimasu, H.*, et al.* (2015). Genome-scale transcriptional activation by an engineered CRISPR-Cas9 complex. Nature *517*, 583-588.

Lai, F., Orom, U.A., Cesaroni, M., Beringer, M., Taatjes, D.J., Blobel, G.A., and Shiekhattar, R. (2013). Activating RNAs associate with Mediator to enhance chromatin architecture and transcription. Nature *494*, 497-501.

Leighton, P.A., Saam, J.R., Ingram, R.S., Stewart, C.L., and Tilghman, S.M. (1995). An enhancer deletion affects both H19 and Igf2 expression. Genes & development *9*, 2079-2089.

Li, W., Notani, D., Ma, Q., Tanasa, B., Nunez, E., Chen, A.Y., Merkurjev, D., Zhang, J., Ohgi, K., Song, X.*, et al.* (2013). Functional roles of enhancer RNAs for oestrogen-dependent transcriptional activation. Nature *498*, 516-520.

Li, W., Notani, D., and Rosenfeld, M.G. (2016). Enhancers as non-coding RNA transcription units: recent insights and future perspectives. Nat Rev Genet *17*, 207-223.

Liu, S.J., Horlbeck, M.A., Cho, S.W., Birk, H.S., Malatesta, M., He, D., Attenello, F.J., Villalta, J.E., Cho, M.Y., Chen, Y.*, et al.* (2017). CRISPRi-based genome-scale identification of functional long noncoding RNA loci in human cells. Science *355*.

Liu, S.J., Nowakowski, T.J., Pollen, A.A., Lui, J.H., Horlbeck, M.A., Attenello, F.J., He, D., Weissman, J.S., Kriegstein, A.R., Diaz, A.A.*, et al.* (2016). Single-cell analysis of long non-coding RNAs in the developing human neocortex. Genome Biol *17*, 67.

Lopes, R., Korkmaz, G., and Agami, R. (2016). Applying CRISPR-Cas9 tools to identify and characterize transcriptional enhancers. Nat Rev Mol Cell Biol *17*, 597-604.

Malik, A.N., Vierbuchen, T., Hemberg, M., Rubin, A.A., Ling, E., Couch, C.H., Stroud, H., Spiegel, I., Farh, K.K., Harmin, D.A.*, et al.* (2014). Genome-wide identification and characterization of functional neuronal activity-dependent enhancers. Nat Neurosci *17*, 1330-1339.

Network, and Pathway Analysis Subgroup of Psychiatric Genomics, C. (2015). Psychiatric genome-wide association study analyses implicate neuronal, immune and histone pathways. Nat Neurosci *18*, 199-209.

Nord, A.S., Blow, M.J., Attanasio, C., Akiyama, J.A., Holt, A., Hosseini, R., Phouanenavong, S., Plajzer-Frick, I., Shoukry, M., Afzal, V.*, et al.* (2013). Rapid and pervasive changes in genome-wide enhancer usage during mammalian development. Cell *155*, 1521-1531.

Pattabiraman, K., Golonzhka, O., Lindtner, S., Nord, A.S., Taher, L., Hoch, R., Silberberg, S.N., Zhang, D., Chen, B., Zeng, H.*, et al.* (2014). Transcriptional regulation of enhancers active in protodomains of the developing cerebral cortex. Neuron *82*, 989-1003.

Quinn, J.J., and Chang, H.Y. (2016). Unique features of long non-coding RNA biogenesis and function. Nat Rev Genet *17*, 47-62.

Rinn, J.L., and Chang, H.Y. (2012). Genome regulation by long noncoding RNAs. Annu Rev Biochem *81*, 145-166.

Roussos, P., Mitchell, A.C., Voloudakis, G., Fullard, J.F., Pothula, V.M., Tsang, J., Stahl, E.A., Georgakopoulos, A., Ruderfer, D.M., Charney, A.*, et al.* (2014). A role for noncoding variation in schizophrenia. Cell Rep *9*, 1417-1429.

Sanjana, N.E., Shalem, O., and Zhang, F. (2014). Improved vectors and genome-wide libraries for CRISPR screening. Nat Methods *11*, 783-784.

Sanjana, N.E., Wright, J., Zheng, K., Shalem, O., Fontanillas, P., Joung, J., Cheng, C., Regev, A., and Zhang, F. (2016). High-resolution interrogation of functional elements in the noncoding genome. Science *353*, 1545-1549.

Sanyal, A., Lajoie, B.R., Jain, G., and Dekker, J. (2012). The long-range interaction landscape of gene promoters. Nature *489*, 109-113.

Savell, K.E., Gallus, N.V., Simon, R.C., Brown, J.A., Revanna, J.S., Osborn, M.K., Song, E.Y., O'Malley, J.J., Stackhouse, C.T., Norvil, A.*, et al.* (2016). Extra-coding RNAs regulate neuronal DNA methylation dynamics. Nat Commun *7*, 12091.

Schaukowitch, K., Joo, J.Y., Liu, X., Watts, J.K., Martinez, C., and Kim, T.K. (2014). Enhancer RNA facilitates NELF release from immediate early genes. Mol Cell *56*, 29-42.

Schizophrenia Working Group of the Psychiatric Genomics, C. (2014). Biological insights from 108 schizophrenia-associated genetic loci. Nature *511*, 421-427.

Shechner, D.M., Hacisuleyman, E., Younger, S.T., and Rinn, J.L. (2015). Multiplexable, locus-specific targeting of long RNAs with CRISPR-Display. Nat Methods *12*, 664-670.

Sigova, A.A., Abraham, B.J., Ji, X., Molinie, B., Hannett, N.M., Guo, Y.E., Jangi, M., Giallourakis, C.C., Sharp, P.A., and Young, R.A. (2015). Transcription factor trapping by RNA in gene regulatory elements. Science *350*, 978-981.

Spieler, D., Kaffe, M., Knauf, F., Bessa, J., Tena, J.J., Giesert, F., Schormair, B., Tilch, E., Lee, H., Horsch, M.*, et al.* (2014). Restless legs syndrome-associated intronic common variant in Meis1 alters enhancer function in the developing telencephalon. Genome research *24*, 592-603.

Telese, F., Ma, Q., Perez, P.M., Notani, D., Oh, S., Li, W., Comoletti, D., Ohgi, K.A., Taylor, H., and Rosenfeld, M.G. (2015). LRP8-Reelin-Regulated Neuronal Enhancer Signature Underlying Learning and Memory Formation. Neuron *86*, 696-710.

Vermunt, M.W., Reinink, P., Korving, J., de Bruijn, E., Creyghton, P.M., Basak, O., Geeven, G., Toonen, P.W., Lansu, N., Meunier, C.*, et al.* (2014). Large-scale identification of coregulated enhancer networks in the adult human brain. Cell Rep *9*, 767-779.

Voisin, S., Almen, M.S., Zheleznyakova, G.Y., Lundberg, L., Zarei, S., Castillo, S., Eriksson, F.E., Nilsson, E.K., Bluher, M., Bottcher, Y.*, et al.* (2015). Many obesity-associated SNPs strongly associate with DNA methylation changes at proximal promoters and enhancers. Genome Med *7*, 103.

Wang, D., Garcia-Bassets, I., Benner, C., Li, W., Su, X., Zhou, Y., Qiu, J., Liu, W., Kaikkonen, M.U., Ohgi, K.A.*, et al.* (2011). Reprogramming transcription by distinct classes of enhancers functionally defined by eRNA. Nature *474*, 390-394.

Yao, P., Lin, P., Gokoolparsadh, A., Assareh, A., Thang, M.W., and Voineagu, I. (2015). Coexpression networks identify brain region-specific enhancer RNAs in the human brain. Nat Neurosci *18*, 1168-1174.

Zovkic, I.B., Paulukaitis, B.S., Day, J.J., Etikala, D.M., and Sweatt, J.D. (2014). Histone H2A.Z subunit exchange controls consolidation of recent and remote memory. Nature *515*, 582-586.